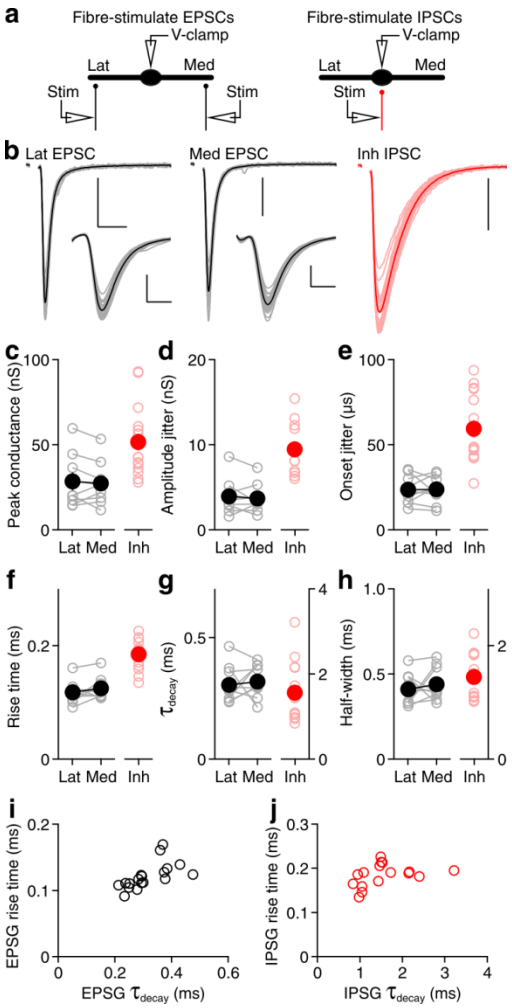

Supplementary Figure 1| Properties of synaptic inputs to mature MSO neurons. (**a**) Schematics of recording configurations for stimulating lateral (Lat, ipsilateral side) and medial (Med, contralateral side) excitatory inputs (left) and a mix of ipsilateral and contralateral inhibitory (Inh) inputs (right, see **Methods**). (**b**) Current traces for example recordings in response to single stimuli of lateral (left) and medial (centre) excitatory inputs (EPSCs) in one recording, as well as an inhibitory input (IPSCs, right) in a different recording. V_m: –75 mV. Light and dark traces represent individual trials and the average response of 30 trials, respectively. Scale bar: 0.5 nA, 2 ms. Insets are zooms of the EPSCs. Inset scale bar: 0.5 nA, 0.5 ms. (**c**–**h**) Average (±s.e.m.) postsynaptic conductance waveforms, calculated from the reversal potential and peak current amplitude were analysed for lateral and medial excitatory inputs to the same neuron (*n*=9 recordings, 18 inputs) and inhibitory inputs to different neurons (*n*=16 recordings, 16 inputs) shown for individual recordings (light markers) and population averages (dark markers) as follows: peak conductance amplitude (**c**), peak amplitude jitter as determined by the s.d. of peak conductance amplitudes (**d**), conductance onset jitter, determined by the s.d. of synaptic delays (**e**), 20–80% conductance rise-time (**f**), decay time constant (τ_{decay}) as determined by single exponential fitting (**g**), and conductance half-width (**h**). Note the additional vertical axis for IPSG analysis in **g,h**. (**i,j**) PSG rise time plotted against decay kinetics, shown for EPSGs (lateral and medial inputs pooled, **i**) and IPSGs (**j**). Although there was a greater diversity of decay kinetics, there was a small positive correlation between rise time and decay kinetics.

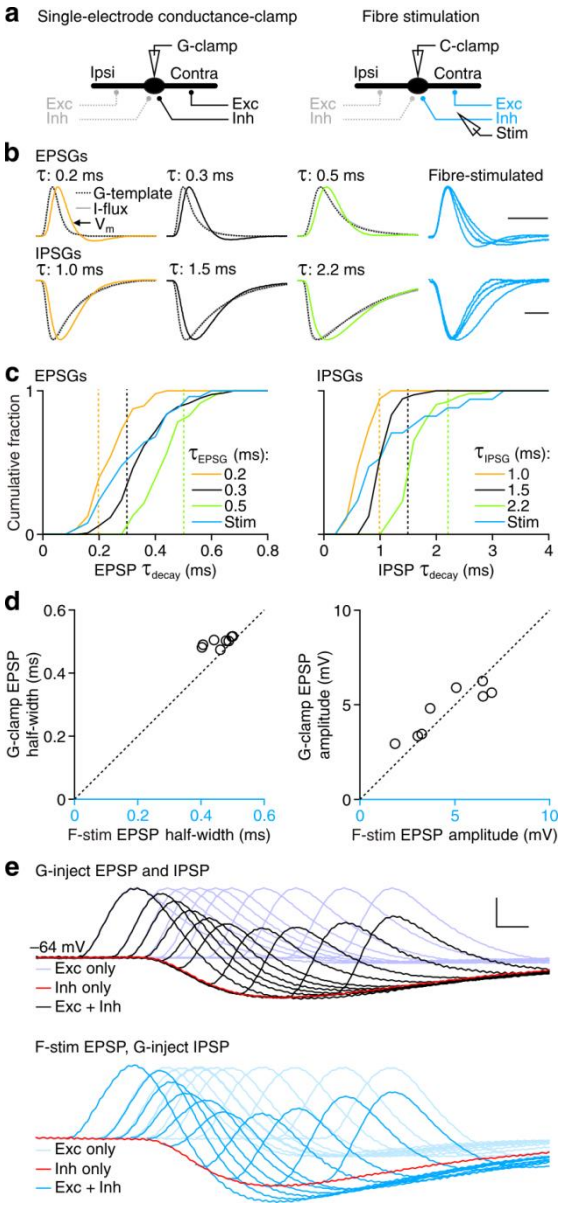

Supplementary Figure 2| Conductance-clamp simulation of EPSPs and IPSPs. (**a**) Schematics of recording configurations for simulating PSPs with conductance-clamp (left) and fibre-stimulating PSPs in current-clamp (C-clamp, right). (**b**) Normalized traces for an example recording showing the transformation of selected excitatory (EPSG, top) and inhibitory (IPSG, bottom) conductance templates into EPSPs and IPSPs, respectively. The conductance command waveforms were measured in **Supplementary Figure 1** (G-command, dotted black traces) and were converted to a current injection command (I-flux, grey traces). Coloured traces indicate the membrane voltage (V_m) from the current injection. Three EPSGs (top) and IPSGs (bottom) were selected from the population to represent fast [τ_{EPSG}=0.2 ms, τ_{IPSG}=1.0 ms (goldenrod)], average [τ_{EPSG}=0.3 ms, τ_{IPSG}=1.5 ms (black)], and slow [τ_{EPSG}=0.5 ms, τ_{IPSG}=2.2 ms (chartreuse)] decay kinetics and are used throughout the manuscript. Normalized example fibre-stimulated EPSPs and IPSPs from separate recordings are shown in blue. Scale bar: 1 ms. (**c**) Cumulative histograms of decay kinetics for PSPs generated by each EPSG (left, *n*=23–26 recordings) and IPSG (right, *n*=24–30 recordings) in the population. Dotted lines indicate the conductance command τ_{decay}. The cumulative distribution of fibre-stimulated EPSPs (*n*=25 recordings) and IPSPs (*n*=17 recordings) are overlaid for comparison (blue). Note that the distributions of stimulated EPSPs and IPSPs cover the range of conductance-clamp-simulated events. (**d**) Comparison between conductance-clamp-simulated and fibre-stimulated EPSP half-width (left) and amplitude (right) measured in the same recording (*n*=7 recordings, from **Fig. 1f–h**). (**e**) Voltage traces from the example recording in **Figure 1f,g** re-plotted, but aligned in time to the IPSP for conductance-clamp-simulated (top) and fibre-stimulated (bottom, stimulus artefacts removed) EPSPs. Although a larger afterhyperpolarization in fibre-stimulated EPSPs indicates a larger recruitment of voltage-gated potassium channels, this observation did not correspond to a significant influence on inhibition-enforced EPSP peak shifts (**Fig. 1h**). Scale bar: 5 mV, 0.5 ms.

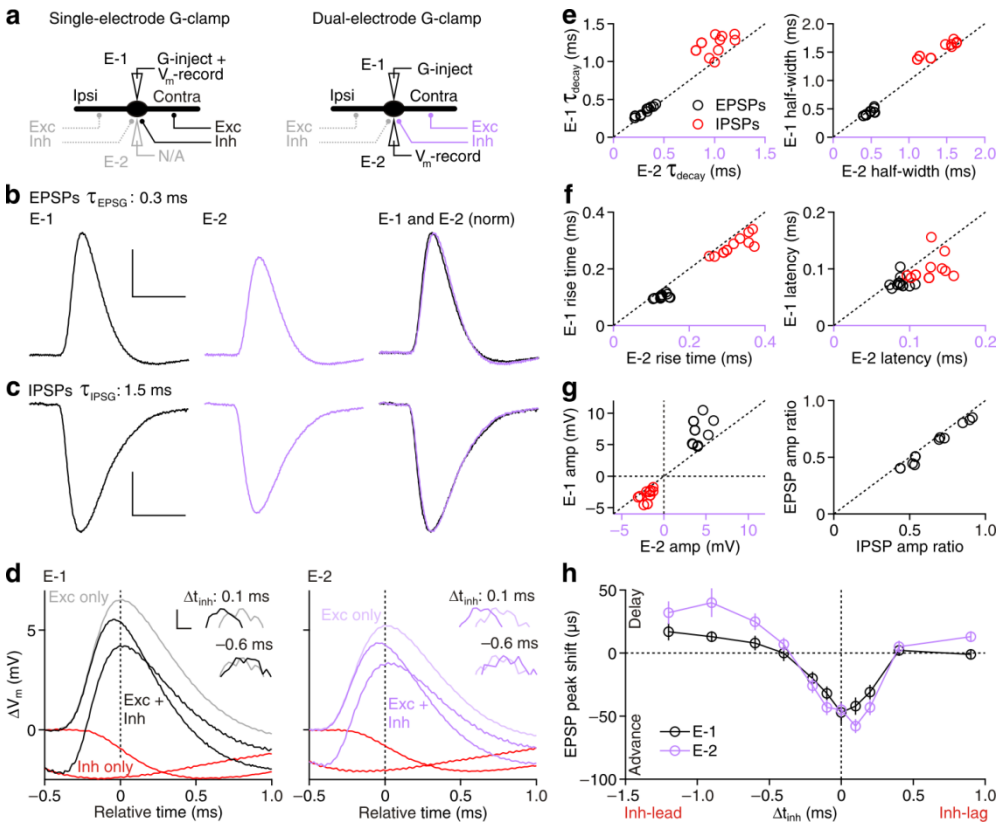

Supplementary Figure 3| Single-electrode and dual-electrode conductance-clamp. (**a**) Schematics of recording configurations for dual-electrode whole-cell recordings. In the same recording, the conductance was always delivered through one electrode (E-1), but the voltage was either measured (V_m-record) in the same electrode (left) or in the second electrode (E-2, right). (**b,c**) Voltage traces of EPSPs (**b**) and IPSPs (**c**) for an example recording, measured in E-1 (left) and E-2 (middle) and normalized (right). V_{rest}: –63 mV. Scale bars: 2 mV, 1 ms (top) and 1 mV, 2 ms (bottom). (**d**) Voltage traces for the recording in **b,c** of inhibition-enforced EPSP peak shifts at timing conditions that advanced (Δt_{inh}=0.1 ms) and delayed (Δt_{inh}=–0.6 ms) EPSP peak timing, as recorded in E-1 (left) and E-2 (right). Insets are zooms of the peaks, aligned in amplitude. Inset scale bar: 0.2 mV, 50 µs. (**e**–**g**) Analyses of EPSP (black) and IPSP (red) E-1 measurements plotted against E-2 measurements for the following parameters: (**e**) decay time constant (left) and half-width (right), (**f**) 20–80% rise time (left) and latency to 20% of peak amplitude (right), and (**g**) PSP amplitude (left). (right) The ratio of E-1:E-2 amplitude for EPSPs is plotted against IPSPs to indicate the linearity of the voltage drop across the electrodes. Note that although there was a consistent voltage drop, the kinetic profile was not altered. (**h**) Average (±s.e.m.) inhibition-enforced EPSP peak shifts plotted against Δt_{inh} for experiments as shown in **d**. For EPSP peak shifts recorded in E-1 and E-2, Δt_{inh}=0.1 ms: –42±7 and –58±6 µs, respectively (P=0.575) and Δt_{inh}=–0.6 ms: 8±6 and 25±7 µs, respectively (P=0.485). Two-way ANOVA, n=10 comparisons from five recording pairs.

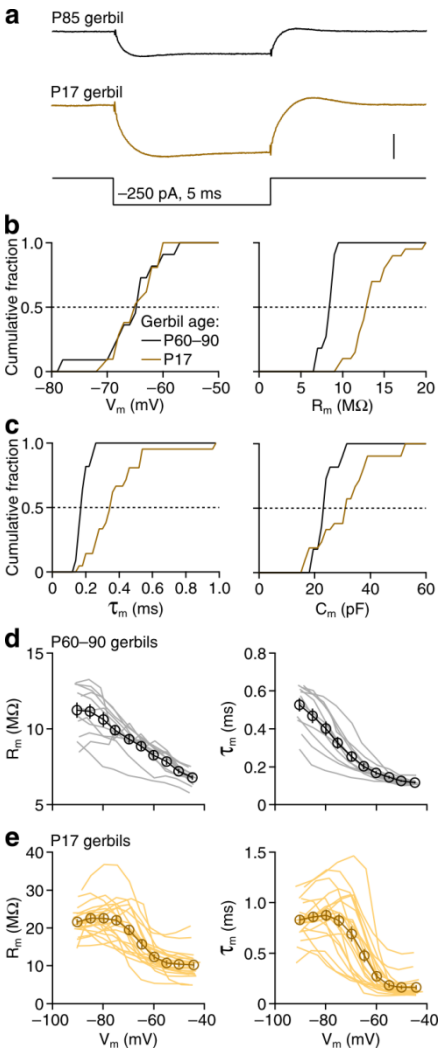

Supplementary Figure 4| Intrinsic membrane properties of P60–90 and P17 MSO neurons. (**a**) Voltage traces for example current-clamp recordings of MSO neurons from a P85 (top) and P17 (bottom) gerbil in response to a –250 pA, 5 ms current step. V_{rest}: –65 (P85) and –65 mV (P17). Scale bar: 2 mV. (**b,c**) Cumulative histograms of resting membrane potential (V_m, **b**, left), membrane resistance (R_m, **b**, right), membrane time constant (τ_m, **c**, left), and membrane capacitance (C_m, **c**, right) for P60–90 (black) and P17 (brown) gerbils. (**d,e**) The voltage-dependence of membrane input resistance (left) and time constant (right) for P60–90 gerbils (*n=11* recordings, **d**) and P17 gerbils (*n*=21 recordings, **e**). Individual recordings and the population average (±s.e.m.) are presented as light lines and dark markers, respectively. Note that the input resistance of some neurons further increased between –80 and –90 mV in P60–90 gerbils, but had completely tapered off by –80 mV in P17 gerbils.

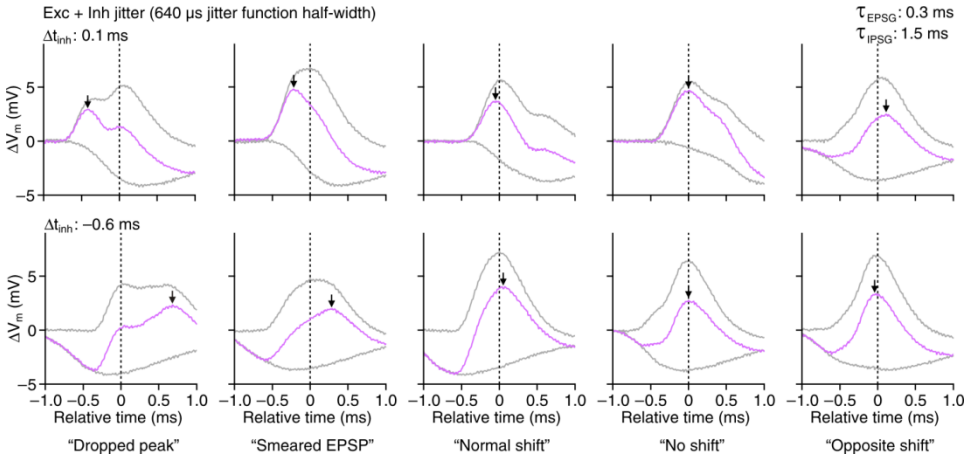

Supplementary Figure 5| Example traces from individual jitter trials. Traces from individual trials for the example recording in **Figure 5c,d**, shown for inhibitory timing conditions that generated an EPSP peak advance (Δt_{inh}=0.1 ms, top) and delay (Δt_{inh}=–0.6 ms, bottom), but with the excitatory plus inhibitory 640 µs jitter function half-width (only voltage traces for the 320 µs jitter function half-width are shown in **Fig. 5d**). Grey traces indicate the EPSP and IPSP alone, and magenta traces indicate the composite PSP. Arrows indicate peak shifts. Examples were chosen to illustrate the diversity of peak shifts observed with substantially jittered EPSPs and IPSPs. (from left to right) A "Dropped peak" occurred when inhibition hyperpolarized one of two distinguishable peaks. A "Smeared EPSP" was more sensitive to peak shifts, consistent with slower EPSPs (**Figs. 2c,e,i,j**, and **3g**). Stochastic timing could also produce a "Normal shift," "No shift" at all, and even an "Opposite shift" of direction the timing condition normally enforced. V_{rest}: –64 mV.

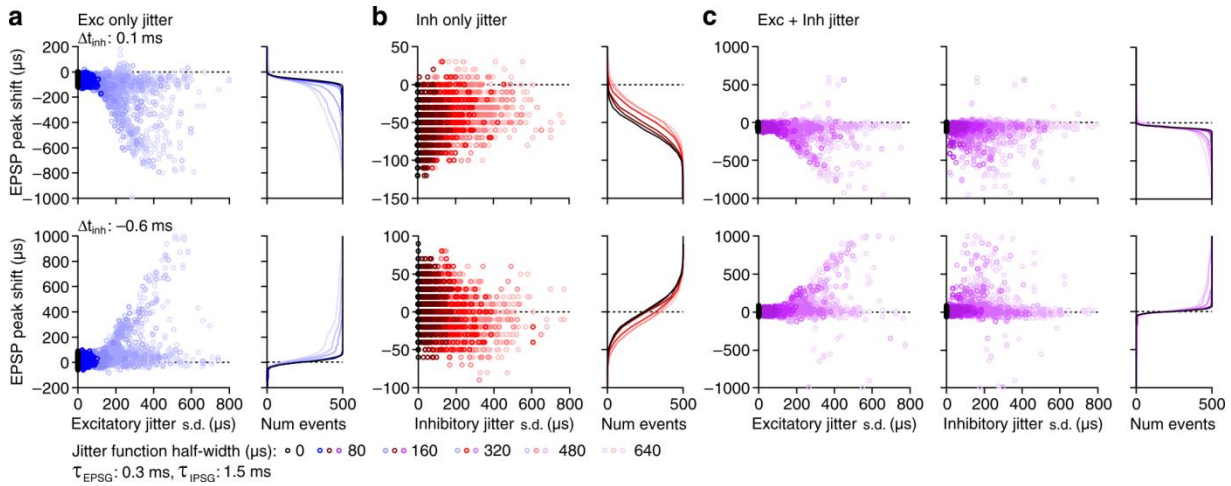

Supplementary Figure 6| Analysis of all jitter trials. All trials for experiments in **Figure 5** were pooled to illustrate the distribution of EPSP peak shifts for each excitatory (**a**), inhibitory (**b**), and excitatory plus inhibitory (**c**) jitter functions. Data are separated for inhibitory timing conditions that enforced an EPSP peak advance (Δt_{inh}=0.1 ms, top) and delay (Δt_{inh}=–0.6 ms, bottom). Data are colour-coded to indicate the amount of jitter for each condition (colour code is indicated below the plots). For each condition, EPSP peak shifts for individual trials are plotted against the s.d. of the four jittered input onset times for that specific trial (left). Note that for excitatory plus inhibitory jitter conditions (**c**) data are plotted independently against the excitatory jitter s.d. (left) as well as inhibitory jitter s.d. (centre). Cumulative histograms are also shown to illustrate the distributions of peak shifts for each jitter function half-width (**a**–**c**, right).

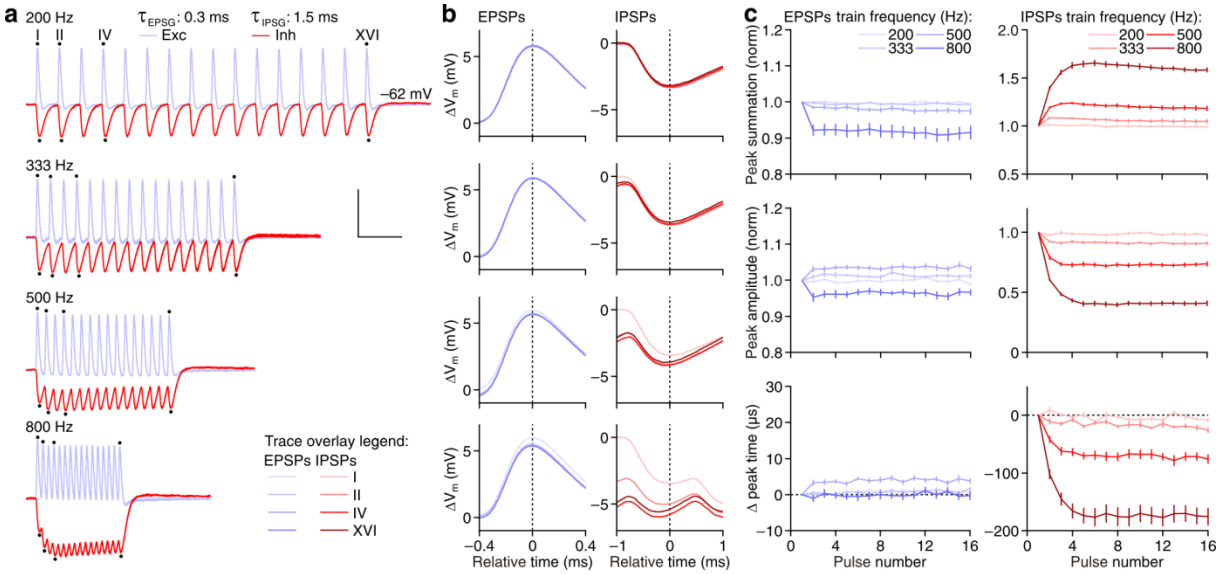

Supplementary Figure 7| Analysis of independent EPSP and IPSP trains. (**a**) Voltage traces for an example 16 pulse train recording of EPSPs (τ_{EPSG}=0.3 ms, blue) and IPSPs (τ_{IPSG}=1.5 ms, red) at (from top to bottom) 200, 333, 500, and 800 Hz. Dots and numerals above the traces indicate individual events that are further analysed in **b**. Scale bar: 5 mV, 10 ms. (**b**) The first, second, fourth, and 16th event for each train in **a** overlaid for EPSPs (left) and IPSPs (right), aligned to the predicted peak time based on the ISI. Traces are colour-coded to indicate their position in the train (colour code is indicated in **a**, bottom right). (**c**) Analysis of each event in EPSP (left) and IPSP (right) trains. (top) Absolute peak amplitude of each event is normalized to the first to indicate summation. At 800 Hz, EPSPs were depressed to 92±2% at the 16th event. IPSP summation begins to develop at 333 Hz. At 800 Hz, IPSPs had summated to 158±2% at the 16th event. (middle) Trough-to-peak amplitude of each event is normalized to the peak amplitude of the first event to indicate the relative voltage modulation throughout the train. At 800 Hz, modulation at the 16th EPSP was 97±1% of the first. IPSP modulations began to deteriorate at frequencies above 333 Hz. At 800 Hz, modulation was reduced to 41±2% at the 16th event. (bottom) Peak time relative to the ISI prediction is plotted to indicate changes in the relative timing of EPSPs and IPSPs. At 500 Hz, EPSPs were delayed by 4±1 µs at the 16th event. IPSPs during the train became advanced at frequencies above 333 Hz, thereby altering the effective Δt_{inh} during the train. At 800 Hz, IPSPs were advanced by 176±15 µs at the 16th event. *n*=8 recordings.

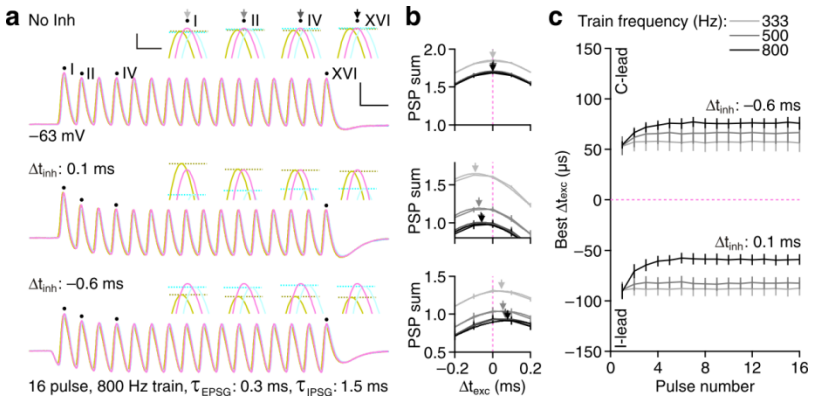

Supplementary Figure 8| Subthreshold PSP summation bias at high frequencies. The protocol and analysis in **Figure 4b,d,h** was repeated, but for 16 pulse trains at 333, 500, and 800 Hz using the average speed EPSG and IPSG. (**a**) Voltage traces for an example recording at 800 Hz without inhibition (top) and with inhibition timed to bias PSP summation toward ipsilateral-leading (Δt_{inh}=0.1 ms, middle) and contralateral-leading (Δt_{inh}=–0.6 ms, bottom) excitation. Traces are colour-coded to reflect excitatory timing conditions as in **Figure 4a**. Dots and numerals above the traces indicate individual events zoomed in insets, as in **Figure 4b,d,f,h**. Scale bar: 5 mV, 2 ms. Inset scale bar: 0.5 mV, 0.1 ms. (**b**) Normalized PSP amplitudes plotted against Δt_{exc} and fitted with Gaussian functions for events indicated by the arrow greyscale tones of the insets in **a**. (**c**) Best Δt_{exc} (±s.d.) plotted against each event in the train at 333, 500, and 800 Hz. At high frequencies, Best Δt_{exc} changes during the train, similarly as for inhibition-enforced EPSP peak shifts (**Fig. 6**). At 800 Hz, the 16th event compared to the first, Δt_{inh}=0.1 ms: –59±5 vs –90±8 µs, P<0.001; Δt_{inh}=–0.6 ms: 64±5 vs 42±4 µs, P<0.001, two-way ANOVA, n=8 recordings. Note that the peak shifts during the train are consistent with an IPSP that becomes relatively advanced in time (**Supplementary Fig. 7**), altering the effective Δt_{inh} during the train.